ARC STRUCTURE IN A COAXIAL MAGNETOPLASMADYNAMIC CHANNEL

Kazunori Mitsuo†, Hirokazu Tahara*, Taro Kimura**

Yoichi Kagaya+ and Takao Yoshikawa++

Division of Mechanical Science, Department of Systems and Human Science,
Graduate School of Engineering Science, Osaka University
Machikaneyama 1-3, Toyonaka, Osaka 560-8531, JAPAN
(E-mail:mitsuo@yoshikawa.me.es.osaka-u.ac.jp)

Abstract

Plasma diagnostic measurement and flowfield analysis were conducted using magneto-plasmadynamic (MPD) channels designed to understand the plasma features and the acceleration processes in the Channel. In order to investigate the dependence of plasma features on the working gases, Ar and H_2 were used as propellants. Current fractions on the electrodes, electron temperature, electron number density in the channel were measured. Current for both gases concentrated intensively near the end of the channel exit. For Ar, there exists a small current concentration near the upstream region above the discharge current of 6 kA. The exhaust Ar ion velocity was also measured with a Fabry-Perot interferometer. The velocities for the MC-III are 4500-7750m/s at a mass flow rate of 0.48g/s and the discharge current of 6-12kA, and increase with the discharge currents. Furthermore, the numerical analysis of axisymmetric MPD flow was conducted to understand the acceleration processes in the MPD channel. As for Ar, the analytical results in the discharge chamber roughly agreed with the experimental ones. Consequently, it is inferred that there exists the strong acceleration zone in the upstream region near the cathode surface.

Nomenclature

B	magnetic field
E	electric field
e	internal energy
j	current density
k_b	three-body recombination rate constant
k_f	ionization rate constant
n	number density
p	pressure
R	gas constant
r	radius
T	temperature
u,v	velocity, (u,v)
θ_{IA}	ionization energy of Ar
θ_{IH}	ionization energy of H
θ_{DH}	dissociation energy of H
ρ	mass density
$\dot{\rho}$	net rate of the ionization or dissociation
μ_0	permeability of free space
σ	electrical conductivity

Subscripts

A	argon
H	hydrogen
e	electricity
g	heavy particle
r	radial coordinate
z	axial coordinate

1. Introduction

The magnetoplasmadynamic (MPD) arcjet is a promising thruster that is developed for exploration missions to deep space, such as Mars, and for raising orbits of large space structures. The MPD arcjet utilizes principally electromagnetic force, i.e., Lorentz force $j \times B$, which is generated by interaction between discharge current and magnetic field azimuthally induced by the discharge current. The thrust depends only on the discharge current and does not basically on propellant species for electromagnetic acceleration. However, in an MPD chamber, complicated chemical reactions involving dissociation and ionization are expected to occur together with the acceleration processes. Furthermore, for acceleration theory of MPD arcjets, there exist two components of electromagnetic force, i.e., the blowing and pumping forces. These forces generate a complicated flowfield in a discharge chamber. Consequently, it has been recognized that the performance characteristics on the discharge voltage, thrust efficiency and electrode erosion depend on propellant species and electrode geometry.

Many researchers have investigated the flowfield in MPD discharge chambers[1]-[4]. However, the

† Research Fellow of the Japan Society for the Promotion of Science, Osaka University.
* Associate Professor, Area of Aerospace Engineering, Graduate School of Engineering Science, Osaka University.
** Graduate Student of Osaka University.
+ Assistant Engineer, Osaka University.
++ Professor, Osaka University

Copyright © 1999 by the Japan Society for Aeronautical and Space Sciences. All right reserved.

plasma acceleration processes are not clarified in detail. To understand the plasma acceleration processes, it is necessary to gather more information of the flowfield in MPD chambers.

In Osaka University, a new research program for understanding of the MPD arcjet acceleration mechanism was started in 1991. It was based on a unique concept that two electromagnetic forces, i.e., the blowing and pumping forces should be independently examined with two different simple discharge chambers. By using simple chamber configurations, plasma diagnostic measurements in the MPD chambers can be easily conducted[5].

In this study, plasma diagnostic measurement and flowfield analysis were conducted using the developed the MPD channel to clarify the acceleration processes in the upstream region of MPD arcjets, where the electromagnetic acceleration is dominant.

In the past experiment, current distributions on the electrodes were examined using a segmented anode and cathode, and electron temperatures and electron number densities were obtained by spectroscopic measurement. Plasma velocities were also measured, using by the Doppler-shift measurement technique. In general, the plasma velocity in an MPD chamber is considered to be about 2000-50000 m/s. The Doppler shift (10^{-3}-10^{-2} nm) measured is too small to evaluate the velocity with a conventional spectroscope. Therefore, in order to measure the plasma velocity, a Fabry-Perot interferometer, which has high spectral resolution performance, was used. In the experiment, the exhaust plasma velocities at the exit of the MPD channel were measured.

Furthermore, the numerical analysis of axisymmetric MPD flow, including non-equilibrium chemical reactions, was conducted in order to compare the experimental results with calculated ones and to understand plasma acceleration processes in the MPD channel.

2. Experimental Apparatus and Operational Condition

2.1 MPD Channel

The coaxial MPD channel (MC-Ⅲ) shown in Fig.1 was designed in order to investigate the MPD channel flow with the experiment and analysis. The straight anode made of copper is 100 mm long and 50 mm in inner diameter, and the rod cathode made of molybdenum is 100 mm long×25 mm in diameter. In measurement of current distributions on the electrodes, both the anode and cathode are divided into five parts, respectively.

The MPD channel are not provided with floating electrodes, and gas is injected uniformly from the upstream end of the discharge chamber. In addition, the downstream end of the electrodes are provided with insulators which prevent current from concentrating on their surfaces of the edge of the MPD channel and from spreading out of the discharge chamber; that is, they are covered with insulators as pumping force does not act in the MPD channel.

Gases are injected from four gas ports into the discharge chamber through a fast acting valve (FAV) fed from a high pressure reservoir. The rise time and the width of the gas pulse, measured with a fast ionization gauge, are 0.5 and 6 msec, respectively. The mass flow rates are controlled by the adjustment of the reservoir pressure and orifice diameter of the FAV.

The main power-supplying pulse forming network, which is capable of storing 62 kJ at 8 kV, delivers a single non-reversing quasi-steady current of maximum 27 kA with a pulse width of 0.6 msec. A vacuum tank 0.6 m in diameter×5.75 m in length, where the MPD channel is fired, is evacuated to some 10^{-2} Pa prior to each discharge.

Ar and H_2 were used as propellants. The mass flow rates are set up at a corresponding critical current of about 8 kA, which is derived theoretically from the role of minimum input power or Alfven's critical ionization velocity[6]. The mass flow rate of Ar and H_2 are 0.48g/s and 0.083g/s, respectively.

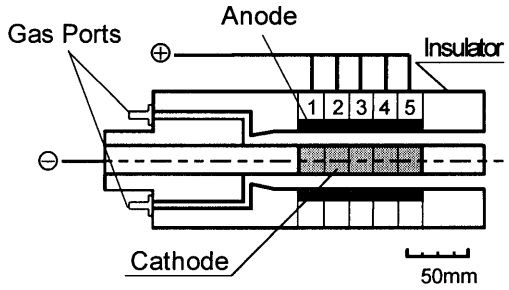

Fig.1 Cross section of MPD MC-Ⅲ.

2.2 Measurement of current fractions on the segmented electrodes

The current entering each electrode segment is measured with a Rogowski coil calibrated with a known shunt resistance in order to examine current fractions on electrodes, that is, to infer the current pattern in the interelectrode region. Current waveforms were measured in the steady-state condition except the transitional state at start of the discharge.

2.3 Spectroscopic measurement

Emission spectroscopic measurement is conducted as reliable plasma diagnostic in the MPD discharge chamber. Light comes from the plasma through a slit 1 mm in width between anode segments. The emission is collected by a lens and introduced into a 0.5-m monochrometer through an optical fiber, as shown in Fig.2. The monochrometer of diffraction-grating-type HAMAMATSU C5095 is provided with 150- and 2,400-grooves/mm grating plates, an image intensifier and a 1024-channel diode array detector, achieving spectral resolutions of 0.8 and 0.05 nm, respectively, per detector channel. The electron temperature is determined using a relative intensity method of spectral lines, i.e., by means of Boltzmann plotting with Ar Ⅱ or N Ⅱ spectral lines. The electron density is estimated from the stark width

of hydrogen H_β line (486.13 nm), in which a mixture of argon or nitrogen and a few percent seed hydrogen is used. Light-of-sight measurement is conducted, and horizontally-average physical properties are calculated directly from the measured horizontally-integrated spectral intensities; i.e., Abel transformations are not carried out.

In optical measurement, the MPD plasma in the channel was examined in a steady-state condition by avoiding transitional phenomena near the start and end of the discharge. The discharge duration time is 1.2 msec, and the emission from plasma is measured for a period of 0.6 msec after 0.4 msec from the discharge ignition. The timing is controlled with a gate of the image intensifier, which can open or close the entrance to the array detector. The emission was measured at six axial points at the middle of the interelectrode.

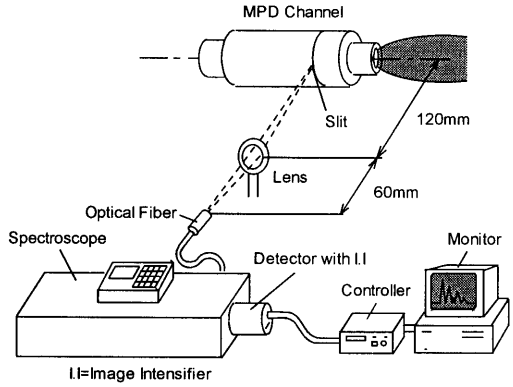

Fig.2 Spectroscopic measurement system.

2.4 Ion velocity measurement

The Doppler shift of MPD channel flow at the present operational conditions are too small to measure that with a conventinal spectroscope. Therefore, in order to measure plasma velocity, a Fabry-Perot interferometer, which has high spectral resolution performance, was used[4].

The spectral line of Ar II (480.6nm) was resolved by the optical system and Fabry-Perot interferometer. The observed spectral line emitted from a particle moving at the speed of u_D is shifted by the Doppler-effect. The frequency difference ($\Delta\nu$) of these lines is

$$\Delta\nu = \frac{u_D}{\lambda_0}\sin\theta \qquad (1)$$

where λ_0 is the wavelength of spectral lines and u_D is the observed plasma velocity. The measured plasma velocity is only streamwise component of the flow velocity.

In the present study, after observing the emission from 30 degree to the steamwise, the emission from perpendicular to the center axis is detected; that is, the measurement was not conducted at the same time. The measurement point was set at the middle of the interelectrodes on the exit plane of the MPD channel. The detail of the experiment is reported in ref.[4].

The exhaust plasma velocity was examined in a steady-state condition by avoiding transitional phenomena near the start of the discharge. The emission from plasma is measured for a period of 0.4 msec after 0.2 msec from the discharge ignition. The timing is controlled with a gate of the image intensifier, which can open or close the entrance to the array detector.

3. Experimental Results

3.1 Current Fractions on electrodes

Figs.3 and 4 show current fractions on the electrodes for Ar and H_2 at the discharge current of 6-10kA. The black and white bar show the current fractions on the cathode and anode, respectively. Current for both gases concentrates intensively near the exit of the channel. For Ar, current flows from the channel entrance to the channel exit at the discharge current of above 6kA, and a small current fraction is observed in the upstream region. However, current for H_2 hardly flows near the upstream region of the channel, and the current fraction in the No.5 anode segment to the total discharge current is over 80 % at every discharge current. This is because the ionization process of H_2 is slower than that of Ar owing to the time lug due to the dissociation process.

3.2 Electron Temperature and Electron Number Density in the MPD channel

Electron temperatures at the middle point of interelectrode for Ar and H_2 are presented in Figs.5 and 6, respectively. Electron temperatures for both gases are hardly dependent on the discharge currents. Electron temperatures for Ar intensively increase near the inlet of the channel and they hardly change from the axial position of 20 mm to the channel exit. On the other hand, electron temperatures for H_2 are almost same in the intermediate region of the channel and increase near the channel exit. In addition, those are below 10000 K in the intermediate region of the channel, and lower than electron temperatures for Ar.

Electron number densities at the middle point of interelectrode for Ar and H_2 are presented in Fig.5 and Fig.6, respectively. Electron number densities for both gases increase gradually from upstream to downstream and also hardly depend on the discharge current.

3.3 Exhaust Plasma Velocity

The plasma (Ar ion) exhaust velocities for the MPD channel MC-III is presented in Fig.7. The measurement point was at the middle point of the interelectrode on the exit of the channel. The solid line illustrated in the figures shows the velocity V_{Th} evaluated from the theoretical electromagnetic blowing thrust. The value of V_{Th} is given as follows:

$$V_{Th} = \left(\frac{\mu_0 J^2}{4\pi} \ln\frac{r_a}{r_c} \right) / \dot{m} \qquad (2)$$

The plasma velocities for the MC-III are 4500-7750m/s at a mass flow rate of 0.48g/s and the discharge current of 6-12kA, and increase with the discharge currents. They are expected to exceed the sonic velocity, if every particle is same temperature and fully ionized. Because the electron temperature near the channel exit is expected to be about 1.5 eV. However, the exhaust velocities at 0.481g/s are smaller than the velocity V_{Th} predicted from the electromagnetic theory.

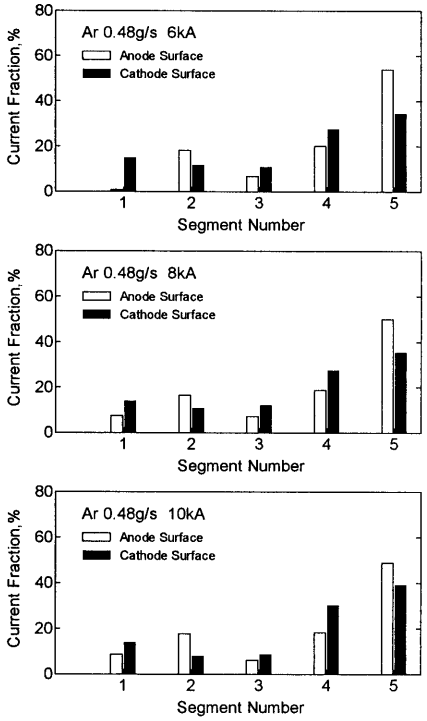

Fig.3 Current fractions on electrodes for Ar.

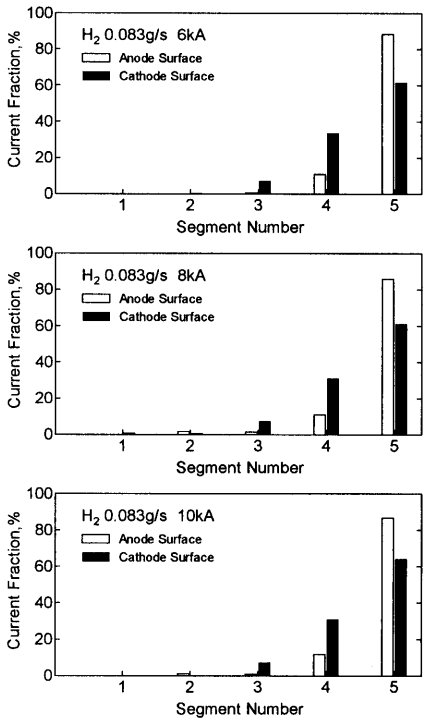

Fig.4 Current fractions on electrodes for H_2.

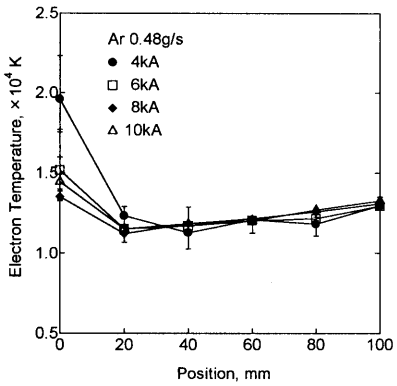

(a)Electron temperature.

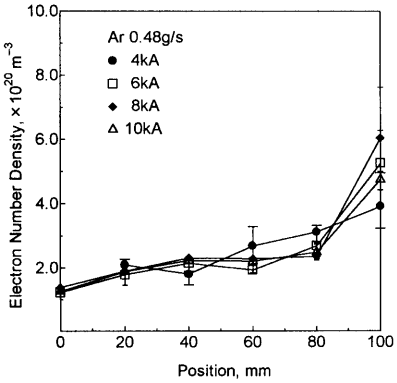

(b)Electron number density.

Fig.5 Axial variations of electron temperature and electron number density for Ar.

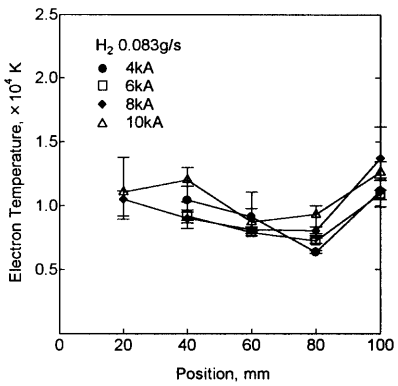

(a)Electron temperature.

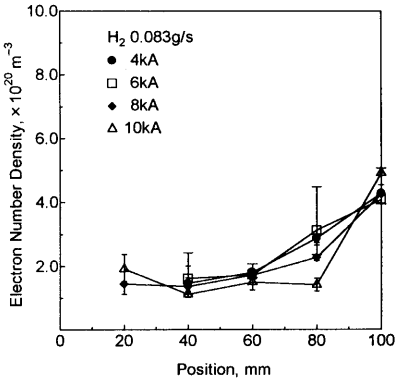

(b)Electron number density.

Fig.6 Axial variations of electron temperature and electron number density for H_2.

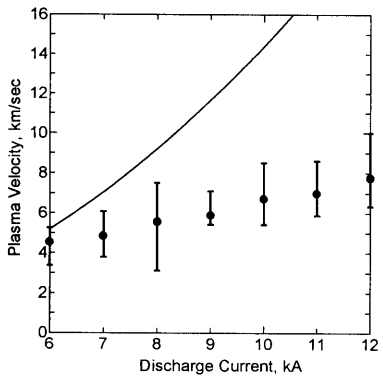

Fig.7 Exhausted velocity of MC-Ⅲ.

4. Numerical analysis

In order to understand the acceleration processes of MPD channel, the numerical simulation of axisymmetric MPD channel flow was conducted. In this calculation, the electrode configuration is the same as MC-Ⅲ[7], [8].

4.1 Assumptions

(1) The working gases are Ar and H_2.
(2) The velocities of electron, ion and neutral are equal.
(4) The all particle(atom, molecule, electron) temperature are equal. In addition, two temperature (electron and heavy particle) model is conducted for Ar.
(3) Non-equilibrium ionization and dissociation processes are considered.
(5) The Hall effect is neglected.
(6) The magnetic field is assumed to have a component in the negative θ -direction.

4.2 Solvers

In solving the flow, the Total Variation Diminishing (TVD)-MacCormack scheme with Roe-Yee-Davis's dissipation term was used. In addition, a point-implicit method was also used in order to stabilize the numerical oscillation, because the present model includes chemical-reaction terms, which are sensitive to the temperature. The induction equation for magnetic field was solved by the successive over relaxation method, and time-dependent term was removed, because we want to get only the steady-state solution. A steady solution was obtained by solving both equations alternatively with coupling them together.

4.3 Governing Equations

Governing differential equations are a group of the modified Euler equations. These equations as described below include equations for electron, atom and global densities, global momentum, energies, and self-consistent magnetic field. The detail of the two temperature model is mentioned in ref.[9].

$$\frac{\partial \mathbf{Q}}{\partial t}+\frac{\partial \mathbf{F}}{\partial z}+\frac{\partial \mathbf{G}}{\partial r}=\mathbf{S} \tag{3}$$

$$\mathbf{Q}=\begin{bmatrix}\rho\\ \rho u\\ \rho v\\ e_t\\ \rho_e\\ \rho_s\end{bmatrix},\quad \mathbf{F}=\begin{bmatrix}\rho u\\ \rho u^2+p\\ \rho uv\\ (e_t+p)u\\ \rho_e u\\ \rho_s u\end{bmatrix},$$

$$\mathbf{G}=\begin{bmatrix}\rho v\\ \rho uv\\ \rho v^2+p\\ (e_t+p)v\\ \rho_e v\\ \rho_s v\end{bmatrix},\quad \mathbf{S}=\begin{bmatrix}-\frac{\rho v}{r}\\ j_r B-\frac{\rho uv}{r}\\ -j_z B-\frac{\rho v^2}{r}\\ \mathbf{j}\cdot\mathbf{E}-\frac{(e_t+p)v}{r}-e_i\\ \dot{\rho}_e-\frac{\rho_e v}{r}\\ \dot{\rho}_s-\frac{\rho_s v}{r}\end{bmatrix}$$

$$\rho=\sum_{s=electron,ion,atom,molecule} m_s n_s \tag{4}$$

$$e_i=\dot{\rho}_e R_A \theta_{IA} \quad (\text{for Ar}) \tag{5}$$

$$e_i=\dot{\rho}_e R_{H_2}(\theta_{IH}+\theta_{DH})+\dot{\rho}_H R_{H_2}\theta_{DH} \quad (\text{for } H_2) \tag{6}$$

The net rate of the ionization is calculated as follows[10]:

$$\dot{\rho}_e=m_{A^+}(k_{IF}n_A n_e-k_{IB}n_{A^+}n_e n_e) \tag{7}$$

$$\dot{\rho}_e=m_{H^+}(k_{IF}n_H n_e-k_{IB}n_{H^+}n_e n_e) \tag{8}$$

The net rate of the dissociation is calculated as follows[10]:

$$\dot{\rho}_H=m_H\left[\sum_s\left(k_{DF,s}n_{H_2}-k_{DB,s}n_H n_H\right)n_s-\left(k_{DF}n_H n_e-k_{DB}n_{H^+}n_e n_e\right)\right]$$

$$(s=e,H^+,H,H_2) \tag{9}$$

The definitions of ionization and dissociation rate are shown below.

$$\alpha=\frac{n_e}{n},\quad \beta=\frac{n_H}{n},\quad n_2=n-\frac{1}{2}(n_e+n_H), \tag{10}$$

The magnetic field equation is given by

$$\frac{\partial B}{\partial t}+\frac{\partial uB}{\partial z}+\frac{\partial vB}{\partial r}$$
$$=\frac{\partial}{\partial z}\left(\frac{1}{\sigma\mu_0}\frac{\partial B}{\partial z}\right)+\frac{\partial}{\partial r}\left(\frac{1}{\sigma\mu_0}\frac{\partial B}{\partial r}\right)+\frac{\partial}{\partial r}\left(\frac{B}{\sigma\mu_0 r}\right) \tag{11}$$

In addition, from Ampere's law and Ohm's law, current density and electric field are described as:

$$j_r = -\frac{1}{\mu_0}\frac{\partial B}{\partial z}, \quad j_z = -\frac{1}{\mu_0 r}\frac{\partial (rB)}{\partial r} \tag{12}$$

$$E_r = \frac{j_r}{\sigma} + uB, \quad E_z = \frac{j_z}{\sigma} - vB \tag{13}$$

Finally, an overall equation of state is required for closure of the set of governing equations:

$$p = \sum_{s=electron,ion,atom,molecule} n_s k_B T_s \tag{14}$$

4.4 Boundary Condition

Discharge current, mass flow rate, degree of ionization, degree of dissociation, and temperature at the inlet of the channel are given as described in table1. They are equal at the radial positions of the channel inlet. In addition, slip-condition was adapted on the electrodes and the working gas is injected with a subsonic velocity.

Table1. Physical properties at the inlet of the MPD channel.

Gas	Ar	H_2
Discharge Current (kA)	8	8
Mass Flow Rate (g/sec)	0.48	0.083
Temperature (K)	5000	5000
Degree of Ionization	0.0005	0.0005
Degree of Dissociation		0.001

5. Calculation Results and Discussion

5.1 Calculation Results

Fig.8 shows the calculated current distributions for Ar and H_2. Current for Ar concentrates near the inlet and outlet of the MPD channel. On the other hand, current for H_2 concentrates intensively near the channel exit and spreads largely out of the channel electrodes end. From the profiles of degree of ionization for both gases, this is because the ionization process of H_2 is slower than that of Ar owing to the time lug due to the dissociation process. Consequently, the electrical conductivity for H_2 is smaller than that for Ar in the upstream region, and current for H_2 intensively concentrate near the channel exit.

Fig. 9 shows the axial velocity in the channel. The plasma for both gases is strongly accelerated near the cathode surface, since the axial electromagnetic force is in inverse proportion to the square of the cathode radius. In addition, the maximum velocity region exists in the downstream from the end of the electrodes, since the plasma in this high pressure region expands to the channel exit.

The plasma for Ar is intensively accelerated in the upstream region near the cathode, where exists the strong axial Lorentz force due to the intense current concentration, as presented in Fig.10. On the other hand, the plasma for H_2 is accelerated near the inlet and outlet of the channel. This is because the slight current flows in the upstream region and Lorentz force acts on the plasma. However, the slight current, as illustrated in the Fig.8(b), was not observed in the experimental result.

5.2 Comparison with Experimental Results

The measured current distributions on the electrodes for both gases roughly agree with analyzed ones, although the intensive current near the channel inlet for Ar was not observed. On the other hand, as for H_2, a small current in the calculated result did not be measured in the upstream region.

Fig.11 shows the measured and calculated temperature at the middle point of the interelectrodes. Calculated temperatures agree with the experimental ones except the inlet of the channel, although calculated temperature is slightly higher than the measured ones.

In addition, two temperature (electron and heavy particle temperature) model was conducted. The electron temperature and heavy particle temperature at the channel entrance was set to 10000 K and 500 K, respectively. Fig.12 shows the calculated electron temperature at the middle point of the interelectrodes. The calculated electron temperature drastically increases near the channel entrance and the tendency of the electron temperature agrees with that of measured one. Accordingly, it is expected that two temperature model need to be available to the MPD flow simulation, although heat conduction should be considered to lower the calculated electron temperature.

Calculated electron number density for Ar also agrees with measured one for the most part. However, that for H_2 is much smaller than measured electron number density. Electron number density is largely dependent on the ionization processes. Therefore, this is because the ionization rates used in tthis simulation model might not be suitable to the MPD channel flow at the present operational condition.

In case of Ar plasma, the calculated results roughly agree with the experimental ones. As a result, it is inferred that there exist the main acceleration zone in the upstream region near the cathode surface, as predicted from the profile of the calculated plasma velocity and Lorentz profile. However, the calculated velocity at the channel exit is about 10000m/s and about twice of the exhausted speed measured with a Fabry-Perot interferometer. In the real MPD flow, current intensively concentrates near the electrode downstream end and spreads in the covered tube. Therefore, it is inferred that plasma is not smoothly accelerated or decelerated in the covered tube due to large Joule heating.

On the other hand, as for H_2, it is inferred from the Lorentz force profile that plasma is strongly accelerated near the electrode end of the MPD channel. However, as remarked above, the ionization reaction model in this calculation should be improved in order to simulate accurately the plasma feature of the MPD channel. In addition, Hall effect needs to be considered in the present calculation, as predicted from the measured current fractions on the electrodes of the MPD channel.

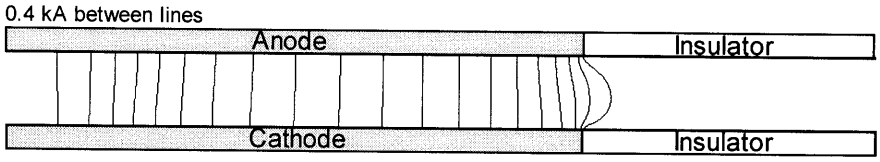

(a)Current distribution for Ar.

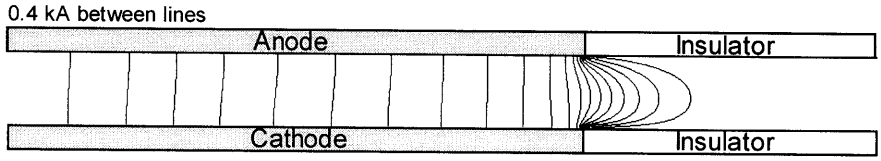

(b)Current distribution for H_2.

Fig.8 Current distribution in the MC-Ⅲ.

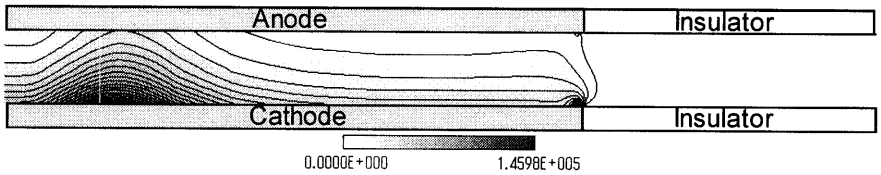

(a)Axial Lorentz force distribution for Ar.

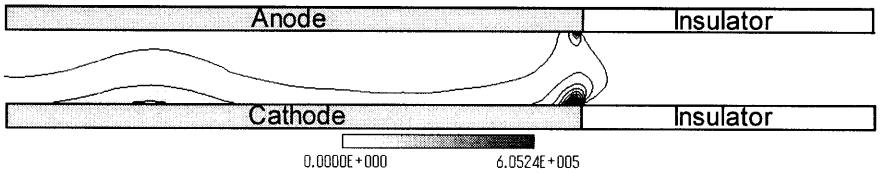

(b)Axial Lorentz force distribution for H_2.

Fig.9 Axial Lorentz force distributions in the MC-Ⅲ.

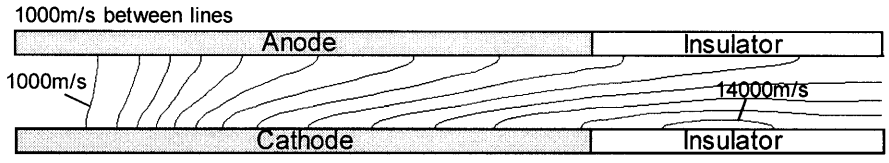

(a)Axial velocity distribution for Ar.

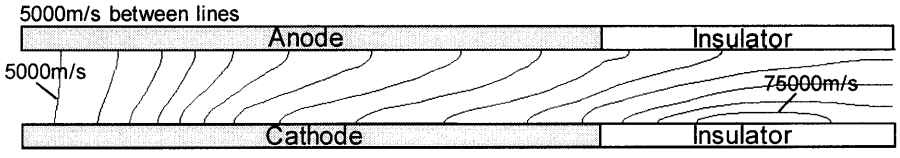

(b)Axial velocity distribution for H_2.

Fig.10 Axial velocity distributions in the MC-Ⅲ.

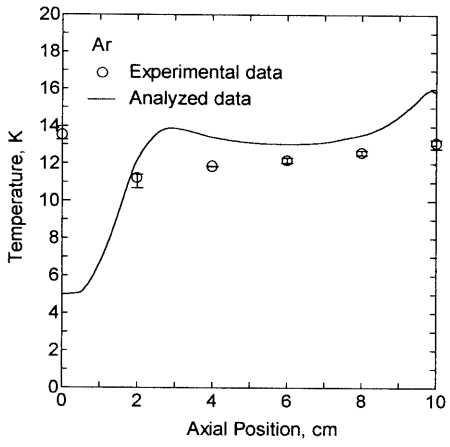

(a)Ar

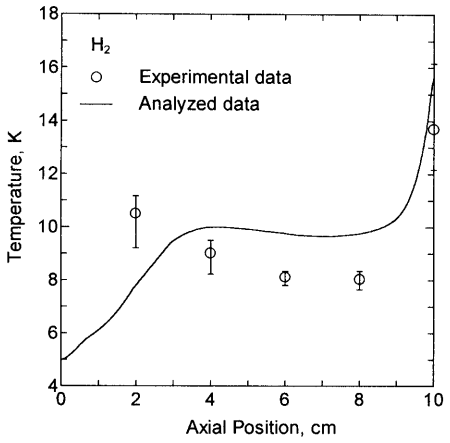

(b)H_2

Fig.11 Measured electron temperature vs calculated temperatures at the middle point of the electrodes.

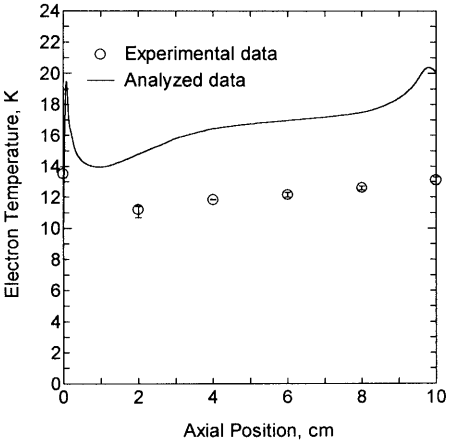

Fig.12 Measured and calculated electron temperatures at the middle point of the electrodes.

6. Conclusions

Plasma diagnostic measurement and numerical analysis were conducted in order to understand plasma features and the acceleration processes in the MPD (magnetoplasmadynamic) channel (MC- Ⅲ). The results are summarized as follows:

(1) Measured current on the electrodes for Ar concentrates near the inlet and outlet of the channel above the discharge current of 6kA. On the other hand, the currents for H_2 concentrate intensively in the downstream region. The Ar ion velocities for the MC-Ⅲ are 4500-7750m/s at a mass flow rate of 0.48g/s and the discharge current of 6-12kA, and increase with the discharge currents. However, the exhaust velocity was about half of the calculated velocity.

(2) The experimental results for Ar in the MPD discharge chamber roughly agreed with calculated ones. Accordingly, it is inferred from the axial Lorentz force profiles that there exists the main acceleration zone in the upstream region near the cathode surface.

(3) Except electron number density, the experimental results for H_2 roughly agreed with calculated ones. From the Lorentz force profile, it is expected that plasma is intensively accelerated in the downstream region near the cathode.

References

[1] Sovey, J. S. and Mantenieks, M. A., "Performance and Lifetime Assessment of Magnetoplasmadynamic Arc Thruster Technology," J. Propulsion and Power, 7 (1991), pp71-83.

[2] Tahara, H., Kagaya, Y. and Yoshikawa, T., "Effects of Applied Magnetic Fields on Performance of Quasisteady Magnetoplasmadynamic Arcjet," J.Propulsion and Power, 11(1995), pp.337-342.

[3] Wegmann, Th., Auweter-Kurtz, M., Habiger, H. A. and Kurtz, H. L., "Experimental Investigation of Steady State High Power MPD Thrusters," AIAA Paper 92-3464, 1992.

[4] Nakayama, T., "Plasma Acceleration Process in the MPD Arcjet", Ph.D Thesis, Tokyo Univ., 1991.

[5]Mitsuo, K., Tahara, H., Hamano, H., Kagaya, Y. and Yoshikawa, T., "Cathode Jet of Magnetoplasmadynamic Thrusters, "IEPC 99-173, 1999.

[6] Alfven, H., "Collision between a Non-ionized Gas and a Magnetized Plasma," Rev. Modern Phy., 32(1960), pp.710-713.

[7]Funaki, I., Toki, K. and Kuriki, K., "Nonequilibrium Flow Analysis of a Two-dimensional MPD Arcjet," IEPC 97-112, 1997.

[8] Niewood, E. H. and Martinez-Sanchez, M., "The Hall Effect in a Numerical Model of MPD Thrusters," IEPC 91-099, 1991.

[9] Mitsuo, K., Tahara, H., Okutani, H., Kagaya, Y. and Yoshikawa, T., "Flowfield in Quasi-Steady Magnetoplasmadynamic Channels," Proceedings of 21st International Symposium on Space Technology and Science, ISTS-98-a-2-07, 1998.

[10]Shoji, T., Ogiwara, K. and Kimura,I., "Analytical Study on Nonequilibrium Flows in Self-Field MPD Thrusters," 23rd International Electric Propulsion Conference, IEPC 93-073, 1993.